

NONLINEAR OPTICAL PHENOMENA

PACS numbers: 42.65.Hw; 42.65.Ky
DOI: 10.1070/QE2004v034n07ABEH002816

Axially symmetric loop phase-conjugation scheme with broadband longitudinally dispersed light beams

V.I. Odintsov

Abstract. **A loop phase-conjugation scheme based on an axially symmetric four-wave interaction of focused light beams is proposed. It is shown that, when a longitudinal dispersion is introduced into the light beams, this scheme allows a phase conjugation of spatially coherent broadband radiation. The region of coherent interaction of focused longitudinally dispersed light beams is estimated.**

Keywords: *phase conjugation, broadband radiation, dispersed light beams.*

1. Introduction

A coherent phase conjugation (PC) of broadband radiation can be achieved using a four-wave interaction (FWI) of intersecting light beams on a large-scale dynamic grating. This interaction takes place, in particular, in a loop PC scheme [1], if the pump beams enter the region of intersection from different sides of a nonlinear medium. However, under ordinary conditions, there is a limitation on the width $\Delta\lambda$ of the radiation spectrum, which is caused by a nonparallelism of the coherence layers of the intersecting beams [2] and can be written as

$$\frac{\Delta\lambda}{\bar{\lambda}} \ll \frac{1}{p\left(N_1^{1/2} + N_2^{1/2}\right)}, \qquad (1)$$

where N_1 and N_2 are the numbers of transverse modes of the two interacting beams with angular divergences $2\theta_1$ and $2\theta_2$ that intersect at an angle ψ; $p = \psi/(\theta_1 + \theta_2)$ characterises the angular separation of the beams; and $\bar{\lambda}$ is the average wavelength.

As was shown in Ref. [2], the limitation on $\Delta\lambda$ can be removed by dispersed light beams. In a dispersed beam, the coherence layers are tilted to the phase fronts and are not perpendicular to the beam axis. At an appropriate angle ψ, this allows the coherence layers of the intersecting beams to be made parallel to each other, thus extending the region of coherent interaction to the entire cross section independently of $\Delta\lambda$. A transparent diffraction grating with a triangle groove profile operating in a single order (or a kinoform instead of it) and a reflecting echelette grating can be used as dispersive elements.

This work shows that, apart from the FWI scheme in intersecting light beams, an axially symmetric scheme with focused beams, whose focal regions have different positions, can be applied. To increase the acceptable radiation spectrum width, longitudinally dispersed light beams can be used in this scheme. A theoretical foundation of this method is presented and its use in the loop PC scheme is considered.

2. Axially symmetric FWI scheme

An axially symmetric FWI scheme for focused light beams is shown in Fig. 1. Here, $L1$ and $L2$ are the counter-propagating focused pump beams, and A_1 and A_2 are the focal points whose positions on the z axis depend on λ. The longitudinal dispersion is introduced into the light beam by the focusing system itself, whose focal distance depends on λ. Waves $R1$ and $R2$ phase-conjugate to the pump beams are generated in nonlinear medium (*1*). A loop PC scheme is realised by introducing a feedback loop along which beams $L1$ and $R2$ return in the form of beams $L2$ and $R1$ from the right into the nonlinear medium. If the feedback loop is absent and the second pump beam $L2$ is injected independently of beam $L1$, an axially symmetric version of the scheme of a two-sided PC mirror is obtained [3]. To obtain a 'classical' FWI with conjugated reference waves $L1$ and $L2$, symbols $L2 \leftrightarrow R1$ in Fig. 1 must be interchanged.

In a general case, the coherence layer is fixed by specifying a certain point S and is determined by the spatial

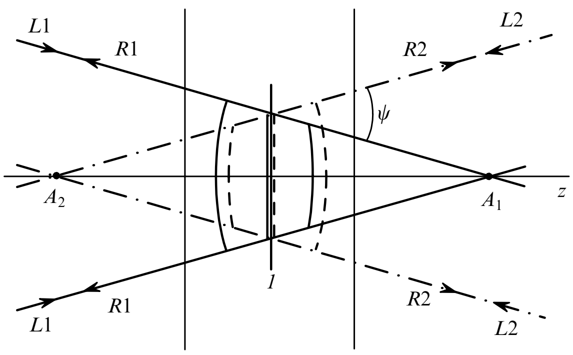

Figure 1. Axially symmetric FWI scheme for focused light beams; (*1*) nonlinear medium.

V.I. Odintsov Department of Physics, M.V. Lomonosov Moscow State University, Vorob'evy gory, 119992 Moscow, Russia;
http://www.phys.msu.su; e-mail: vodintsov@mtu-net.ru

Received 3 November 2003; revision received 13 April 2004
Kvantovaya Elektronika **34** (7) 639 – 643 (2004)
Translated by A.S. Seferov

distribution of the absolute value of the complex degree of coherence, which is calculated in terms of the fields at points S and $P(x, y, z)$: $|\gamma_{SP}| = |\gamma_S(x, y, z)|$. The position and curvature of the coherence layer is determined from the maximum-coherence surface that passes through point S. If the focal length is independent of λ and no longitudinal dispersion is introduced, the coherence layers then coincide with the phase fronts and turn out to be different for beams $L1$ and $L2$ (because they are focused differently). Correspondingly, the coherence layers for beams $L1$ and $R2$ and for $L2$ and $R1$ do not coincide in space. The greater angle ψ (see Fig. 1), which must be sufficiently large for separating the beams with allowance for their irregular angular divergence, the larger the degree of mismatch of the coherence layers.

At different curvatures of the coherence layers, an efficient coherent interaction over their entire cross sections is possible only if their thickness, determined by the radiation coherence length $l_c = \bar{\lambda}^2/\Delta\lambda$, is large enough; this imposes a certain limitation on $\Delta\lambda$. This limitation has the same form (1) as for intersecting unfocused beams, if ψ corresponds to the angle shown in Fig. 1, and θ_1, θ_2 are the irregular beam angular divergences in the plane of coincidence of their cross sections. If a longitudinal dispersion is introduced, the coherence layers of beams $L1$ and $L2$, as well as those of $R1$ and $R2$, can be brought into coincidence within a certain spatial region. The coincidence of the coherence layers of dispersed beams $L1$ (solid lines) and $L2$ (dash–dotted lines) is illustrated in Fig. 1.

The spatial coherence and the area of coherent interaction of longitudinally dispersed light beams will be considered in the next section for the case of focusing systems with a linear optical power $\Phi = a + b\lambda$ (a and b are numerical coefficients), which do not disturb the spatial coherence of a light beam. 'Linear' focusing systems are: a raster 'flat lens' and a kinoform lens ($a = 0$), an achromatic lens composed of thin lenses in contact ($b = 0$), and also any of their combinations. As to an ordinary lens, the nonlinearity of its refractive index $n(\lambda)$ determines a nonlinearity $\Phi(\lambda)$ and the presence of a dispersion of the radiation group velocity, which restricts the coherence area in the focused-beam cross section. Under such conditions, when $n(\lambda)$ is approximated by the Cauchy formula, the acceptable spectrum width is $\Delta\lambda/\lambda \approx [(\Delta\lambda/\lambda)_a]^{1/2}$, where $(\Delta\lambda/\lambda)_a$ is the acceptable spectrum width in the absence of dispersion (the same relationship is also valid for intersecting unfocused beams, if an ordinary prism is used as a dispersive element).

3. Spatial coherence of focused longitudinally dispersed light beams

Let the field of the initial unfocused beam in front of the focusing system be strictly spatially coherent and have a flat coherence layer oriented normally to the z axis. This field can be represented as the sum of spatially coherent $E(\boldsymbol{\alpha})$ fields changing in correlation with time, each of which is a superposition of plane waves with wave-vector components $\boldsymbol{k}_\perp = \boldsymbol{\alpha}$ perpendicular to the z axis [2]. The field of the focused beam is represented as a superposition of partial fields appearing upon focusing of individual $E(\boldsymbol{\alpha})$ fields.

Let a one-dimensional set of focal points (centres of spherical waves) appearing upon the incidence of a single $E(\boldsymbol{\alpha})$ field on a linear focusing system and the partial field associated with them be denoted as $A_F(\boldsymbol{\alpha})$ and $E_F(\boldsymbol{\alpha})$, respectively, where $F = \{a, b, z_0\}$ characterises the position and parameters of the focusing system, and z_0 is the coordinate of its centre (point O) lying on the z axis. Figure 2 shows the focal points appearing when two $E(\boldsymbol{\alpha})$ fields with vectors $\boldsymbol{\alpha} = 0$ (points A_1, A_2, A_3) and $\boldsymbol{\alpha} = \boldsymbol{\alpha}'$ (points A'_1, A'_2, A'_3) are incident on the focusing system. All of the focal points of set $A_F(\boldsymbol{\alpha})$ lie on a common straight line running through point $\hat{C}$ common for such sets. We assume that the fields related to individual focal points, the partial fields, and the total field are defined over an unbounded free space. When calculating the degree of coherence, the changes in the field incident on the focusing system as functions of the time and transverse coordinates are considered as steady-state random Gaussian processes.

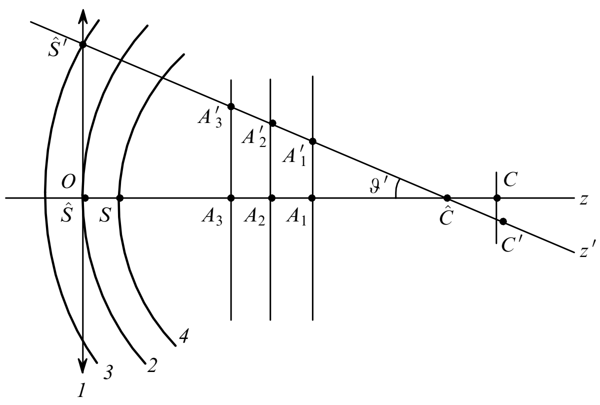

Figure 2. Focusing of $E(\boldsymbol{\alpha})$ fields by the focusing system: (*1*) focusing system; (*2*) sphere of spatial coherence ($\boldsymbol{\alpha} = 0$); (*3*) sphere of spatial coherence ($\boldsymbol{\alpha} = \boldsymbol{\alpha}'$); (*4*) spherical field-coherence layer centred at point C; and (C') centre of the coherence layer of field $E_F(\boldsymbol{\alpha}')$ correlated with layer (*4*).

3.1 Spatial coherence of partial fields

Consider coherent properties of a partial field $E_F(0)$ (fields with $\boldsymbol{\alpha} \neq 0$ are treated similarly). The coordinates of the focal points $A_i(\lambda)$ on the z axis are determined by the expression

$$z(\lambda) = z_0 + \frac{1}{a + b\lambda}. \tag{2}$$

Summing the fields associated with the centres of spherical waves $A_i(\lambda)$, we find that, within the framework of the paraxial approximation, the resulting field $E_F(0)$ is rigorously spatially coherent on a sphere with a radius $\hat{R} = 1/a$. The point of intersection $\hat{S}$ of this sphere with the z axis has a coordinate $z(\hat{S}) = z_0$ and thus coincides with the centre O of the focusing system. The centre of the sphere of spatial coherence is located at point $\hat{C}$ (Fig. 2). The set of focal points for which there exists a sphere of spatial coherence is called a coherent set.

Consider the coherence layers of the partial field $E_F(0)$ taking point S lying on the z axis (Fig. 2). If S coincides with point $\hat{S}$, the coherence layer then coincides with the sphere of spatial coherence. When point S is shifted from this sphere, the transverse size of the coherence area D_c^0 of the partial field $E_F(0)$ becomes bounded. Within D_c^0, the coherence layer is, to within a satisfactory accuracy, a sphere with centre C on the z axis and a radius

$$R = \frac{\rho_1\rho_2}{(\hat{\rho}_1\hat{\rho}_2/\hat{R}) - d}, \quad (3)$$

where $\rho_i = \hat{\rho}_i - d$; $\hat{\rho}_i = z[A(\lambda_i)] - z(\hat{S})$; $i = 1, 2$; $d = z(S) - z(\hat{S})$; $\lambda_1 = \bar{\lambda} - \Delta\lambda/2$; and $\lambda_2 = \bar{\lambda} + \Delta\lambda/2$.

The diameter of the circle at the central part of the focused-beam cross section, at the edges of which the degree of coherence falls to a specified value $|\gamma|$, is

$$D_c^0 = 2K_0\frac{1}{|\bar{\hat{q}}|}\frac{\bar{\lambda}}{\Delta\lambda}(\bar{\lambda}|\bar{\hat{\rho}}|)^{1/2}\frac{|1-\bar{\hat{\xi}}|^{3/2}}{|\bar{\hat{\xi}}|^{1/2}}, \quad (4)$$

where $K_0 = 2(\pi^{-1}\ln 2)^{1/2}[(1/|\gamma|^4) - 1]^{1/4}$; $\bar{\hat{\rho}} = \hat{\rho}(\bar{\lambda})$; $\bar{\hat{q}} = (\hat{R} - \bar{\hat{\rho}})/\hat{R}$; and $\bar{\hat{\xi}} = d/\bar{\hat{\rho}}$. The intensity distribution in λ is assumed to be Gaussian. It is also assumed that the distance from point S to focal points is not too short.

The partial fields $E_F(\boldsymbol{a})$ at $\boldsymbol{a} \neq 0$ have similar properties. In Fig. 2, focal points A'_1, A'_2, and A'_3 form a coherent set whose sphere of spatial coherence with the centre at point $\hat{C}$ intersects the z' axis at point $\hat{S}'$. Angle ϑ' is found from the relationship $\tan\vartheta' = (|\boldsymbol{a}'|/2\pi)(a/b)$.

3.2 Spatial coherence of the total field E

The coherence layers of different partial fields are called correlated if the time-dependent partial fields in these layers correlate with one another. It can be shown that all of the coherence layers touching common arbitrary auxiliary sphere with the centre at point $\hat{C}$ are correlated. This touching takes place at points of intersection of this sphere and $z(\boldsymbol{a})$ axes (Fig. 2).

An actual beam incident on a focusing system has a limited diameter D_L. Let the focused beam be characterised by an opening angle 2φ for the mean wavelength $\bar{\lambda}$ and a diameter $D_L(\bar{\xi}) = 2|\bar{\rho}(\bar{\xi})|\varphi = 2|\bar{\hat{\rho}}||1-\bar{\hat{\xi}}|\varphi$ (here, $\bar{\hat{\xi}} = d/\bar{\hat{\rho}}$) (Fig. 3). Figure 3 also shows the angle χ between the normal to the sphere of spatial coherence and the normal to the phase front for $\lambda = \bar{\lambda}$ at point P located at the beam edge. The angles φ and χ are related by the exprerssion $\chi = \varphi|\bar{\hat{q}}|$.

A disturbance of the spatial coherence of the total field E within the geometrical bounds of an actual focused beam can be caused by two factors: a disturbance of the spatial coherence of the E-constituting partial fields and a spatial noncoincidence of the correlated coherence layers of these fields. By using expression (4), we can show that the partial fields within the bounds of an actual focused beam remain spatially coherent at rather long distances from the focusing system comparable with its focal length. When calculating the spatial coherence of the total field E within the limits of such distances, we may take into account only the second factor – the spatial noncoincidence of the correlated coherence layers for different partial fields. Due to this factor, the spatial coherence of field E in the cross section of an actual beam is disturbed already at much shorter distances from the focusing system than this happens for individual partial fields. The possibility of ignoring a disturbance in the spatial coherence of individual partial fields appreciably simplifies calculations and generally justifies the use of the partial-field method.

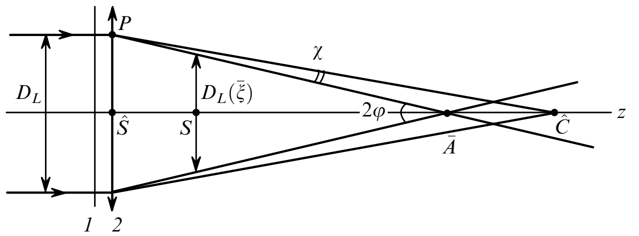

Figure 3. Angular aperture 2φ of the focused beam and angle of inclination χ of the coherence layer relative to the phase front: (*1*) coherence layer for the initial beam; (*2*) focusing system; $\hat{S}S = d$; $\bar{A} = A(\bar{\lambda})$; $\hat{S}\bar{A} = \bar{\hat{\rho}}$; $S\bar{A} = \bar{\rho}$; and $\bar{\hat{\xi}} = d/\bar{\hat{\rho}}$.

The noncoincidence of the correlated coherence layers is determined by their nonconcentric profile increasing with $|d|$. As the distance from the sphere of spatial coherence increases, the centre of curvature of the coherence layer of partial field $E_F(\boldsymbol{a})$ shifts from point $\hat{C}$ and moves along the $z(\boldsymbol{a})$ axis. Point C in Fig. 2 is the centre of the coherence layer of partial field $E_F(0)$ (this layer passes through point S), and point C' is the centre of the coherence layer of partial field $E_F(\boldsymbol{a}')$ correlated to it.

In contrast to D_c^0, we determine the cross-sectional size D_c of the total-field coherence area by specifying the condition

$$\gamma_E = \left(\overline{|\gamma_{SP}|^2}\right)^{1/2}$$

at its boundary. Here, point S is taken on the beam axis, and the bar means the averaging over the realisation of the actual spatial structure of the field incident on the focusing system. The following representation of the time-dependent changes in partial fields $E_F(\boldsymbol{a})$ at a given point $\boldsymbol{r}$ of the light beam was used to calculate γ_{SP}. Let a random complex function $f(t)$ describe changes in fields $E_F(\boldsymbol{a})$ with time in correlated coherence layers touching an arbitrarily chosen auxiliary sphere with the centre at point $\hat{C}$ (see above). As can be easily shown, the change in field $E_F(\boldsymbol{a})$ with time in the coherence layer passing through point $\boldsymbol{r}$ is then described by a function $f[t - \tau(\boldsymbol{a}, \boldsymbol{r})]$, where $\tau(\boldsymbol{a}, \boldsymbol{r}) = h(\boldsymbol{a}, \boldsymbol{r})/u$ is the time shift, $h(\boldsymbol{a}, \boldsymbol{r})$ is the distance between the points of intersection of the $z(\boldsymbol{a})$ axis with this coherence layer and the auxiliary sphere, and u is the group velocity of radiation in the medium, which is assumed to be independent of λ.

The calculation of γ_E was performed assuming that the frequency and angular spectra of radiation incident on the focusing system have Gaussian profiles. It has shown that the coherence layers of the total field E virtually coincide with those of the partial field $E_F(0)$. The expression obtained for D_c is

$$D_c = 2K\frac{l_c}{\theta|\bar{\hat{q}}|}\frac{(1-\bar{\hat{\xi}})^2}{|\bar{\hat{\xi}}|}, \quad (5)$$

where $K = \sqrt{2}\pi^{-1}\ln 2\,(\gamma_E^{-4} - 1)^{1/2}$.

3.3 Mutual coherence of two focused dispersed beams with correlated coherence layers

Along with a disturbance of the spatial coherence of each of the interacting beams considered above, the length of the area of the coherent FWI is also affected by perturbations of the spatial coincidence of the coherence layers of different beams.

Let us analyse beams $L1$ and $L2$ in the form of partial fields at $\boldsymbol{a} = 0$, and let the spheres of spatial coherence for these beams coincide with each other. For definitiveness, we assume that $L2$ can be produced by reflecting beam $L1$ from a spherical mirror coinciding with the sphere of spatial coherence. The coherence layers of beam $R2$ phase conjugate to $L2$ coincide with those of $L2$. This allows us to further analyse beam $R2$, which directly interacts with almost parallel beam $L1$, instead of $L2$. If this interaction is taken into account, the coherence layers of $R2$ turn out to be correlated with those of $L1$.

If the correlated coherence layers of beams $L1$ and $R2$ coincide on the common sphere of spatial coherence, then, as the distance from it increases, a difference in the curvatures of these layers determined from (3) appears. As a result, the difference in the positions of the correlated coherence layers that coincide on the z axis increases, as the beam periphery is approached.

The correlation factor of interacting fields $L1$ and $R2$ at point P is defined by the expression

$$\gamma_{\text{int}}(P) = \frac{\overline{A_{L1}(P,t)A^*_{R2}(P,t)}}{\left[\overline{|A_{L1}(P,t)|^2}\right]^{1/2}\left[\overline{|A_{R2}(P,t)|^2}\right]^{1/2}}, \qquad (6)$$

where A_{L1} and A_{R2} are generatrices and the overbars denote the time averaging.

By specifying the value of $|\gamma_{\text{int}}|$ at the boundaries of the area of coherent interaction of beams $L1$ and $R2$, we obtain its cross-sectional size

$$D_{\text{c}}^{\text{int}} = 2K_{\text{int}} \frac{(l_{\text{c}}|\bar{\rho}|)^{1/2}}{|\bar{q}|^{3/2}|\bar{\xi}|} \left| \left[1-(1-\bar{q})\bar{\xi}\right]^2 - \bar{q}^2\bar{\xi}^2 \right|, \qquad (7)$$

where

$$K_{\text{int}} = \frac{(\ln 2)^{1/4}}{\sqrt{\pi}} \left(\ln \frac{1}{|\gamma_{\text{int}}|} \right)^{1/4}.$$

Here, parameters $\bar{\rho}$, $\bar{q}$ and $\bar{\xi}$ refer to one of the two interacting beams. If they are replaced by the parameters of the other beam, $D_{\text{c}}^{\text{int}}$ remains unchanged. Expression (7) was derived under the assumption that each of the interacting beams was spatially coherent.

For $\hat{R} = \infty$, when $\bar{q} = 1$, the dependence of $D_{\text{c}}^{\text{int}}$ on $\bar{\xi}$ is symmetrical relative to the spatial-coherence plane. Let the beams' positions be identical to those in Fig. 1. We then have $\bar{\xi} > 0$ in a region of $D_{L1} < D_{R2}$, and $D_{\text{c}}^{\text{int}}$ thus must be compared to D_{L1}; at $\bar{\xi} < 0$, on the contrary, $D_{R2} < D_{L1}$ and $D_{\text{c}}^{\text{int}}$ must be compared to D_{R2}. In view of an obvious symmetry, it is sufficient to analyse one of these regions.

Figure 4 shows $D_{\text{c}}^{\text{int}}$ as a function of $\bar{\xi}$ at $\bar{q} = 1$ for $\bar{\xi} > 0$. Here, we have introduced $M_{\text{int}} = K_{\text{int}}(l_{\text{c}}|\bar{\rho}|)^{1/2}$ and $D_{L1} < D_{\text{c}}^{\text{int}}$ if $\bar{\xi} < \bar{\xi}_{\text{c}}$, where $\bar{\xi}_{\text{c}} = (\varphi/\tilde{\varphi}_{\text{int}} - 1)^{-1}$ at $\varphi > \tilde{\varphi}_{\text{int}}$ and $\bar{\xi}_{\text{c}} = \infty$ at $\varphi < \tilde{\varphi}_{\text{int}}$; and $\tilde{\varphi}_{\text{int}} = K_{\text{int}}(l_{\text{c}}/|\bar{\rho}|)^{1/2}$. The quantity $2\tilde{\varphi}_{\text{int}}$ determines the angular aperture of the region of coherent interaction of beams in the far-field zone. Similar results for $\boldsymbol{\alpha} \neq 0$ can also be obtained for $E_F(\boldsymbol{\alpha})$ fields.

In the region $0 < \bar{\xi} < 1$, the disturbance of a coherent interaction of two beams, caused by different radii of curvature of their coherence layers, and a disturbance of the spatial coherence of an individual beam considered above are characterised under typical conditions by comparable d values. Therefore, when determining the extension of the region of the coherent FWI, both of these factors must be taken into account.

Concluding this section, let us briefly discuss the transformation of focal points, spheres of spatial coherence, and

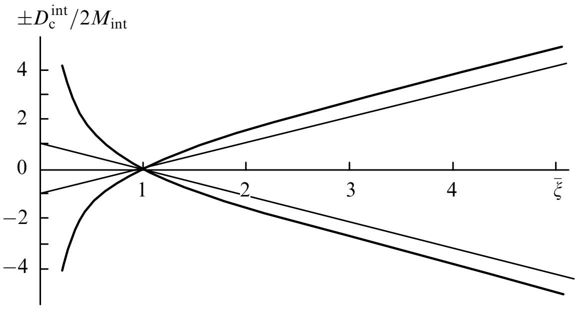

Figure 4. $D_{\text{c}}^{\text{int}}$ as a function of $\bar{\xi}$.

coherence layers of partial fields by an achromatic optical system. A coherent system of focal points also forms a coherent system. The point of intersection of its sphere of spatial coherence with the system's axis and the centre of this sphere are, respectively, the images of point $\hat{S}(\boldsymbol{\alpha})$ (points $\hat{S}$ и $\hat{S}'$ in Fig. 2) and point $\hat{C}$ for the initial partial field. Points $S(\boldsymbol{\alpha})$ and $C(\boldsymbol{\alpha})$ characterising the coherence layers of the initial partial field are transformed similarly: the corresponding points for the coherence layers of the transformed field are their images.

4. Loop PC scheme

Figure 5 shows one of possible versions of the axially symmetric loop PC scheme with longitudinally dispersed pump beams. The beam paths for the incidence on kinoform lens (*1*) are shows for only one monochromatic plane wave L. As a result of the passage of a light beam through lens (*1*) and achromatic lens (*2*), a focal point A^+ appears. Since the focal length for kinoform lens (*1*) is $f_1 \propto 1/\lambda$, the position of A^+ on the system's optical axis depends on λ. Achromatic lens (*4*) forms a weakly converging beam $L1$ in a cell with nonlinear medium (*5*). The second pump beam $L2$ is produced by the reflection of beam $L1$ from flat mirror (*6*) [other returning systems can also be used instead of (*6*)]. After passing through lens (*4*), the beam is focused at point A^- and, except for its small central part, is shut by diaphragm (*3*). Wave $R2$ phase-conjugate to pump beam $L2$ is generated at the left boundary of the nonlinear medium and, being reflected by mirror (*6*), is transformed into wave $R1$ phase-conjugate to pump beam $L1$. Both pump beam $L1$ and $R1$ pass through the hole in diaphragm (*3*).

The fraction of the beam $L2$ intensity transmitted through this hole is

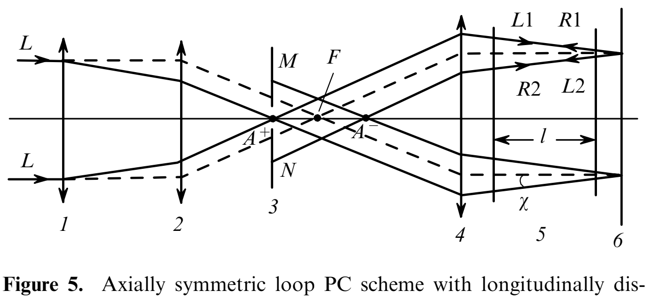

Figure 5. Axially symmetric loop PC scheme with longitudinally dispersed light beams: (*1*) long-focus kinoform lens; (*2*,*4*) confocal achromatic lenses with a common focus at point F; (*3*) diaphragm; (*5*) nonlinear medium; and (*6*) flat mirror.

$$\eta = \left(\frac{2r_{\rm d}}{MN}\right)^2 \approx \frac{\mu^2}{4}\left(\frac{1}{p}+\frac{\Delta\lambda}{2\bar{\lambda}}\right)^2 \approx \frac{\mu^2}{4p^2}, \quad (8)$$

where $2r_{\rm d}$ is the hole diameter; $p = \chi/\theta$; 2θ is an irregular angular divergence for mirror (*6*); χ is the angle shown in Fig. 5; $\mu = r_{\rm d}/(f_2\theta_1)$; f_2 is the focal length for lens (*2*), and $2\theta_1$ is the angular divergence of the beam incident on kinoform lens (*1*). For $p = 5$ and $\mu = 2.2$ (the intensity of the beam with a Gaussian angular spectrum incident from the left decreases by $\sim 3\,\%$), we obtain $\eta \approx 5\,\%$.

The focal length $\bar{f}_1$ of lens (*1*) at a wavelength $\bar{\lambda}$ is related to the diameter D_L of the beam incident on it through the formula

$$\bar{f}_1 = \frac{D_L}{2p\theta_1} = \frac{\pi D_L^2}{4p\bar{\lambda}\sqrt{N}}$$

(N is the number of transverse modes). By varying the magnification Y of the telescopic system of lenses (*2*) and (*4*), it is possible to change the beam diameter D on mirror (*6*) ($D = D_L Y$) and parameter $\bar{\rho} = D/2\chi = \bar{f}_1 Y^2$. Since the coherent-interaction length calculated according to (5) and (7) is proportional to D^2, changes in D must involve changes in the medium length $l \propto D^2$.

Let us make numerical estimates for $\Delta\lambda/\bar{\lambda} = 5\times10^{-2}$, $N = 2000$, and $p = 5$. For simplicity, we take into account only the length of coherent interaction of L and R beams, since, for the selected parameters, the spatial coherence of individual beams is disturbed at long distances. By specifying $|\gamma_{\rm int}| = 0.7$ at the beam boundary, we obtain $\bar{\xi}_{\rm c} = 0.27$. For $\bar{\lambda} = 10^{-4}$ cm and $D = 1$ cm, we have $\bar{\rho} = 35$ cm; the coherent-interaction length $d_{\rm c} = \bar{\xi}_{\rm c}\bar{\rho}$ that limits the length l of the nonlinear medium is then ~ 9 cm.

By using the stimulated-scattering nonlinearity and assuming $l = d_{\rm c}$, we obtain the threshold pump power $P_L = p\bar{\lambda}\sqrt{N}/(\beta\bar{\xi}_{\rm c})$, where β is the specific stimulated-scattering gain. At $\beta \approx 10^{-3}$ cm MW^{-1} (the Raman and Kerr nonlinearities), $P_L \approx 80$ MW. One should expect much lower threshold powers when using the saturation nonlinearity in dyes, if $\bar{\lambda}$ corresponds to the short-wavelength wing of a broad absorption line [6].

5. Conclusions

Bringing into coincidence the coherence layers of dispersed light beams for extending the region of their coherent interaction may be applied not only in broadband coherent PC radiation but also in other problems of nonlinear optics and holography (note that, at the FWI, the coincidence of the coherence layers of the interacting beams is necessary even at a short relaxation time of the dynamic grating, which is smaller than the inverse width of the spectrum). In addition, introducing a dispersion allows a superposition of ultrashort pulses in intersecting or differently focused laser beams.

In contrast to a transverse dispersion that produces an asymmetric light beam, a longitudinal dispersion preserves the axially symmetric beam geometry. Axially symmetric PC schemes exclude an angular deviation of the emerging PC beam from the incident pump beam under arbitrary conditions, including a pump-depletion mode. In order not to reduce the PC quality in axially symmetric schemes, it is desirable to use only those types of nonlinearity for which the relaxation time of the dynamic grating is independent of its spatial period.

When a dispersed beam propagates, the larger the difference of the coherence layers from the phase fronts, the quicker the process of disturbing the spatial coherence. This disturbance far exceeds the disturbance of the spatial coherence for a nondispersed beam. Therefore, much attention in this work is given to the calculation of coherent properties of focused dispersed beams. The use of the partial field method allowed us to obtain simple analytic expressions characterising the spatial coherence and the region of the coherent interaction of focused longitudinally dispersed beams.

By using longitudinally dispersed beams, a ring achromatic interference pattern similar to achromatic strips in Refs [2, 4, 5] can be obtained. It can also be observed with spatially incoherent light beams produced by splitting one and the same initial beam and differing in the positions of their focal regions. In this case, introducing a longitudinal dispersion makes it possible to bring into coincidence the identical layers of the both beams [5]. When ordinary lenses are used for focusing, visibility dips similar to those observed in Refs [2, 5] must be formed in the ring interference pattern.

References

1. Odulov S.G., Soskin M.S., Khizhnyak A.I. *Lazery na dinamicheskikh reshetkakh* (Lasers on Dynamic Gratings) (Moscow: Nauka, 1990) Ch. 4.
2. Odintsov V.I., Sokolova E.Yu. *Kvantovaya Elektron.*, **21**, 778 (1994) [*Quantum Electron.*, **24**, 723 (1994)].
3. Sternklar S., Weiss S., Segev M., Fisher B. *Opt. Lett.*, **11**, 528 (1986).
4. Ditchburn R. *Fizicheskaya optika* (Physical Optics) (Moscow: Nauka, 1965) p. 127.
5. Odintsov V.I., Sokolova E.Yu. *Opt. Spektrosk.*, **85**, 273 (1998).
6. Nikolaev D.A., Odintsov V.I. *Kvantovaya Elektron.*, **20**, 1130 (1993) [*Quantum Electron.*, **23**, 983 (1993)].